Proceedings of the ASME 2013 International Mechanical Engineering Congress and Exposition
IMECE2013
November 15-21, 2013, San Diego, California, USA

IMECE2013-63773

COMPREHENSIVE ANALYSES OF NUCLEAR SAFETY SYSTEM CODES

Glenn A. Roth
University of Idaho
Idaho Falls, ID, USA

Fatih Aydogan
Professor
University of Idaho
Idaho Falls, ID, USA

Many nuclear system codes have been developed for the main purpose of analyzing reactor performance of a nuclear power plant system during steady state and transient conditions. These codes generally include power plant component models for pumps, pipes, steam generators, pressurizers and other components. The parallel development of these nuclear system codes has been supported by government laboratories, universities, private entities and other organizations throughout the world. This has resulted not only in multiple codes, but multiple versions of the same code with different capabilities. The development paths of each code version have been driven by specific needs. The challenge for the user is to select a code that performs well for the desired analysis problem. Therefore, this work compares different aspects of various nuclear system codes. Firstly, it compares the governing equations for mass, momentum and energy in the evaluated system codes. Secondly, it compares all the codes' closure models. Closure models are used in system codes to model thermal and mechanical non-equilibrium as well as the coupling of the phases. Thirdly, it compares the Separate Effect Tests (SET) and Integral Effect Tests (IET) employed for the verification and validation (V&V) during the development of each system code. These comparisons cover several thermal and hydraulic models, such as heat transfer coefficients for various flow regimes, two phase pressure correlations, two phase friction correlations, drag coefficients and interfacial models between the fields. Fourthly, major assumptions about the governing and closure equations in these codes are compared and discussed. Fifthly, numerical approach of every code is benchmarked with each other since numerical approach not only affects the speed of the system codes but also the accuracy of the results. Sixthly, the limitations of the codes are evaluated because these codes are challenged by analyzing not only existing nuclear power plants, but also next generation nuclear power plants. The nuclear industry is developing new, innovative reactor designs, such as Small Modular Reactors (SMRs), High-Temperature Gas-cooled Reactors (HTGRs) and others. Sub-types of these reactor designs utilize pebbles, prismatic graphite moderators, helical steam generators, innovative fuel types, and many other design features that may not be fully analyzed by current system codes. The results of this work serve as a guide for development of these system codes and indicate areas where models must be improved to adequately address issues with new reactor design and development activities.

INTRODUCTION

Nuclear reactor systems are complex, and require detailed analysis to evaluate reactor performance during normal operations as well as accident or transient conditions. Computer codes that are used to analyze these complex reactor systems are called "system codes".

System codes are used to evaluate both design basis and beyond-design-basis accidents. They can be used to evaluate steady-state performance of reactor systems, and are also used for transient analyses. The system codes can aid reactor system engineers in refueling evolutions, relicensing efforts with regulatory agencies, and the applications for reactor plant power uprating. System codes are also widely used in the design of nuclear plant systems.

System codes include detailed models of reactor components, such as pipes, pressurizers, valves, and pumps. These hydrodynamic models have frequently been extended to

include a code capability to model multiple phase flows. The interaction between coolant phases is modeled to capture heat transfer properties between the phases, and mass exchange between those phases. Components that model heat transfer through materials, as well as nuclear heat generation are also part of system code analyses. System codes also include basic control elements that can be used to implement reactor control systems such as pump trips, reactor scrams, and other automated system responses.

This paper compares and contrasts the capabilities, performance, and validation of many of the modern system codes, such as RELAP, TRAC, TRACE, COBRA/TRAC, RELAP/SCDAP, CATHARE, and ATHLET.

Code performance is characterized by many factors. This paper compares the codes based on conservation models, closure relations, numerical solution methods, code limitations, and simplifying assumptions.

CONSERVATION MODELS

Detailed comparisons between the codes include a discussion of the conservation equations in each of the codes. The conservation models are important in the development of the interaction between phases and the balancing of mass, momentum, and energy.

The conservation equations are used in all the system codes considered in this work. The solution methods and closure relationships for these equations vary, but the basic equations for conservation of mass, momentum and energy are consistent across the codes. These equations are shown below:

Mass Conservation:

$$\frac{\partial}{\partial t}(\alpha_k \rho_k) + \frac{1}{A}\frac{\partial}{\partial x}(\alpha_k \rho_k v_k A) = \Gamma_k \tag{1}$$

Where:
α_k = Void fraction of phase k
ρ_k = Density of phase k
A = Area between phases
v_k = Velocity of phase k
Γ_k = Generation rate of phase k

Momentum Conservation:

$$\begin{aligned}&\alpha_k \rho_k A \frac{\partial v_k}{\partial t} + \frac{1}{2}\alpha_k \rho_k A \frac{\partial v_k^2}{\partial x} = -\alpha_k \rho_k B_x A \\ &-(\alpha_k \rho_k A) FW_k \bullet v_k + \Gamma_k A (v_{kI} - v_k) \\ &-(\alpha_k \rho_k A) FI_k \bullet (v_k - v_r) \\ &-C\alpha_k \alpha_r \rho_m A\left[\frac{\partial (v_k - v_r)}{\partial t} + v_r \frac{\partial v_k}{\partial x} - v_k \frac{\partial v_r}{\partial x}\right]\end{aligned} \tag{2}$$

Where:
B_x = Body force in x coordinate direction
FW_k = Wall drag coefficient for phase k
FI_k = Interphase drag coefficient for phase k
v_r = Velocity of phase r
v_{kI} = Velocity of phase k at the interface
ρ_m = Density of phase mixture

Energy Conservation:

$$\begin{aligned}&\frac{\partial}{\partial t}(\alpha_k \rho_k U_k) + \frac{1}{A}\frac{\partial}{\partial x}(\alpha_k \rho_k U_k v_k A) = \\ &-P\frac{\partial \alpha_k}{\partial t} - \frac{P}{A}\frac{\partial}{\partial x}(\alpha_k v_k A) + Q_{wk} + Q_{ik} \\ &+\Gamma_{ig} h_k^* + \Gamma_w h_k' + DISS_k\end{aligned} \tag{3}$$

Where:
U_k = Specific internal energy for phase k
P = Wetted perimeter
Q_{wk} = Wall heat transfer per unit volume to phase k
Q_{ik} = Interface heat transfer per unit volume to phase k
Γ_{ig} = Vapor generation rate due to energy exchange in the bulk fluid
Γ_w = Vapor generation rate due to energy exchange at the wall
h_k^* = Specific enthalpy in phase k
h_k' = Specific enthalpy for interface mass transfer in the thermal boundary layer
$DISS_k$ = Energy dissipation function of phase k

The mass, momentum, and energy conservation equations can be written for each phase in the system. Doing this for the vapor and liquid phases results in the so-called six-equation model.

Figure 1 shows a characteristic hydraulic system that illustrates the challenges in modeling two-phase hydrodynamic systems. The conservation equations model the exchange of mass, energy, and momentum between the phases, but do not explicitly model the entrained droplets or vapor bubbles.

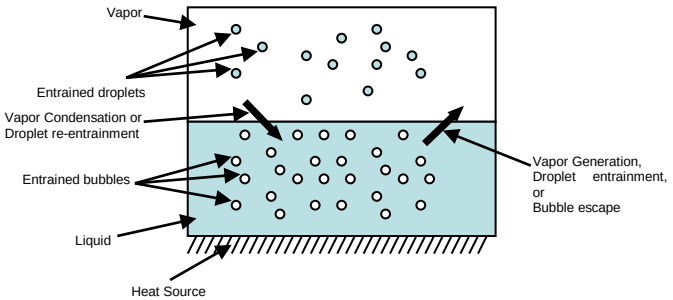

Figure 1 - Generic Two-Phase System

The following sections will discuss specific differences between some of the system codes.

RELAP-7 is currently under development at the Idaho National Laboratory (INL). Consequently, it does not

incorporate conservation models for more than two phases. The RELAP-7 code has governing equations (mass, momentum, and energy) for the liquid phase only. The work is ongoing to incorporate governing equations for the vapor phase, as outlined in Reference [1].

The RELAP5 codes (MOD3, MOD3.3, 3D, SCDAP) use the six conservation equations for the hydrodynamic system. These codes add two more mass conservation equations. One is used to track the mass of dissolved solute in the liquid coolant (usually boron), and the other is used to track noncondensible gasses in the vapor phase. It is assumed in each code that the velocity, temperature and pressure of the solute and noncondensible gasses are the same as the related phase. This simplifies the system solution, since it is not necessary to add energy and momentum conservation equations to track the dissolved solute and gasses. However, the liquid energy equation is modified when noncondensible gasses are included. RELAP5-3D and RELAP5-3D/SCDAP include a third additional mass balance equation to track radionuclides.

The six equation model is also used in the CATHARE code. The mass, momentum, and energy conservation equations are written for the vapor and liquid phases. Up to two transport equations can be added for noncondensable gasses. As before, the noncondensable gasses are assumed to be at the same temperature and move with the same velocity as the vapor phase. Thus, only the mass conservation equation is needed for the noncondensable gasses.

TRACE also uses the six equation model, solving the conservation of mass, momentum and energy equations for each phase in the coolant. TRACE includes the capability to model noncondensable gasses that move at the same velocity and have the same temperature as the vapor/gas phase. Thus, the noncondensible gasses can be modeled with a single mass-conservation equation. As with RELAP, dissolved boron can also be tracked in the TRACE code, subject to the assumption that the boron mass does not affect the liquid momentum equation, and it does not affect the thermodynamic or other physical properties of the liquid. Boron tracking is enabled by use of a model for solubility of boric acid. Additional solutes (besides boron) could be modeled if the user provides a different solubility curve (through a user option).

The COBRA-TRAC code uses a three-field representation of two-phase flow in the 3D vessel component. The three fields are gas/vapor, continuous liquid, and entrained liquid (droplet) [2]. The gas/vapor field includes noncondensible gasses as well as vapor resulting from boiling. The entrained liquid field captures the droplets that may be entrained in the vapor/gas flow. The 1D components use the familiar six equation model with a seventh equation to capture the mass conservation of the noncondensible gas phase. As before, there are two equations for conservation of mass, momentum, and energy, one for each phase (liquid or vapor/gas).

The ATHLET code offers two different models for hydrodynamic simulation. The first model is called the five-equation model, and has separate mass and energy conservation equations for two phases (liquid and vapor) and a single momentum equation for the phase mixture. This assumption neglects the phase interface shown in Figure 1, which makes it impossible to compute separate phase velocities. The results from this model provide a coolant mass flow rate instead of a velocity. The five-equation model also has mixture level tracking capability. The second model is a standard six-equation model with mass, momentum and energy conservation equations for both phases. The mixture level tracking is not available in the six-equation model. In the annular and annular-mist flow the water phase is split into two fields, one for droplets, the other for liquid film.

CLOSURE RELATIONS

Closure relations provide additional equations to make the conservation equations mathematically solvable. The closure relations provide information about the heat transfer rates between phases, heat transfer coefficients between phases and the walls, the viscous shear in the flow, mass exchange among fields at the phase boundaries, momentum exchange at the phase interfaces, drag forces at the solid boundaries, turbulence terms in the continuous fields, droplet entrainment and de-entrainment, and other information. The correlations are also used to determine which flow regime is present. The point of Critical Heat Flux (CHF) is used to distinguish between flow regimes that have liquid in contact with the wall and those that are experiencing dryout, and there is little or no liquid contact with the wall. Figure 2 shows the vertical flow regimes that are pre-CHF. Stratified, horizontal, pre-CHF flow regimes are shown in Figure 3. Vertical post-CHF flow regimes are depicted in Figure 4, which also shows the upper and lower "quench fronts" where the walls are re-wetted.

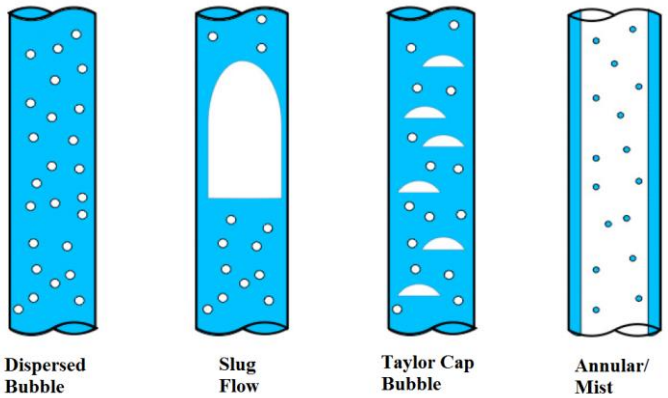

Figure 2 – Vertical Pre-CHF Flow Regimes [14]

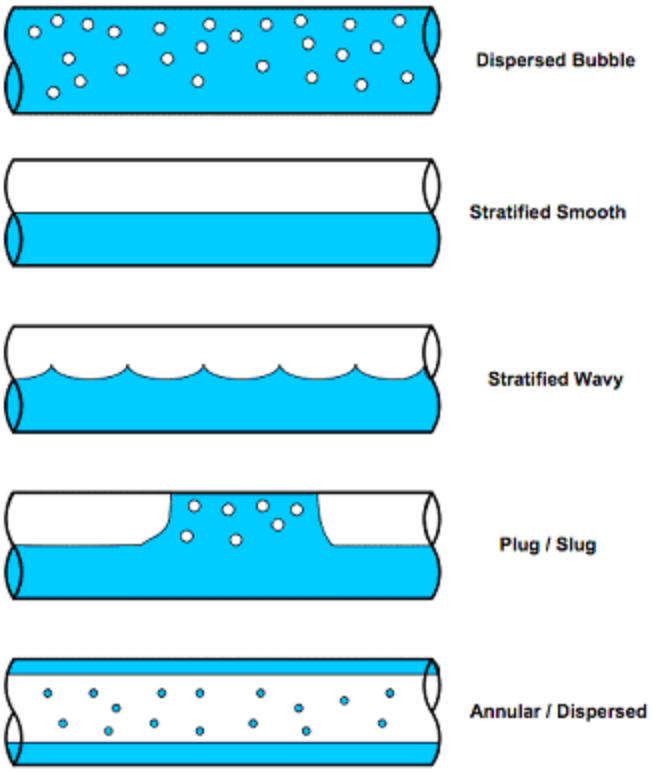

Figure 3 - Horizontal flow regimes [14]

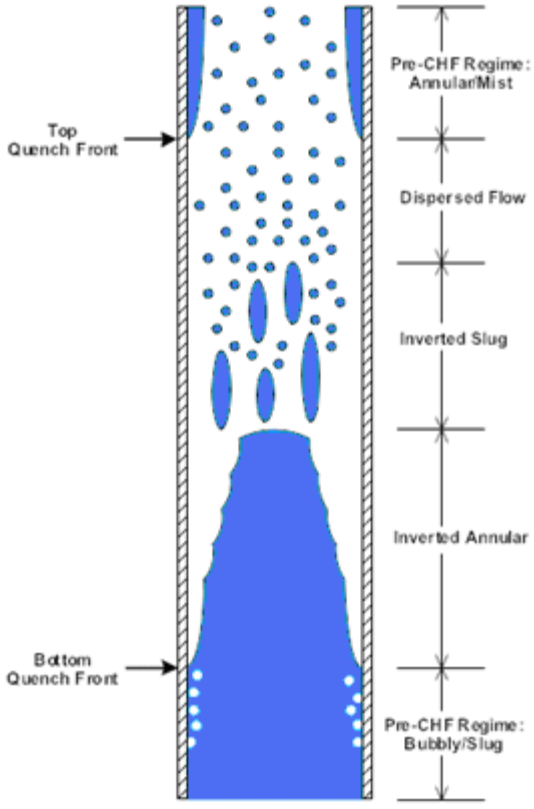

Figure 4 - Inverted flow regimes for post-CHF [14]

Averaging (volume and time) is typically used to simplify the solution procedure of the six equations. The closure relations are also used to compensate for information that is lost during the averaging process. It is clear from this discussion that the closure relationships can affect the analysis results in significant ways. The six-equation model is very similar between the analysis codes, differing principally in numeric solution to the system of equations. The closure relationships determine the key parameters that are required for solution of the conservation equations. The following sections discuss details of the closure relations used in the compared system codes.

Mass and Energy Closure Relationships

Interfacial Heat Transfer: The bulk interfacial heat transfer in the RELAP5-3D code actually involves both heat and mass transfer between the phases. The heat transfer is computed based on temperature gradients between each phase and the interface. The interface temperature is assigned to be the saturation temperature for the local pressure. Correlations for heat transfer on each side of the interface are included in the code. Both superheated and subcooled conditions are allowed for each phase, so heat transfer can be in either toward or away from the interface for each phase. All of the thermal energy transferred to the interface from either side contributes to vaporization. This is then used to compute the mass transfer to the vapor/gas phase. Similarly, all of the heat conduction away from the interface contributes to condensation, and can be used to compute the mass transferred to the liquid phase. The net rate of mass transfer is determined by summing the contributions from each side of the interface.

The heat transfer coefficient that is used between the phases in the bulk flow of the coolant depends on the flow regime. Therefore, detailed flow regime maps have been developed for use in RELAP5-3D, with different heat transfer correlations for each regime. The vertical and horizontal flow regime maps for RELAP5 are shown in Figure 5 and Figure 6, respectively.

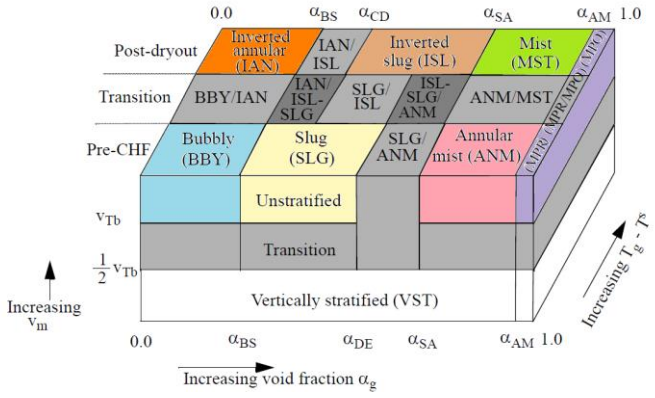

Figure 5 – RELP5 Vertical Flow Regime Map [33]

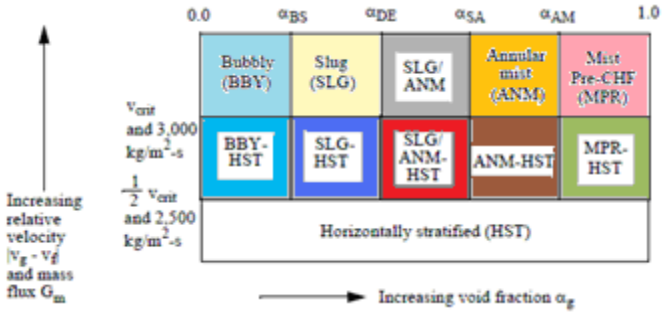

Figure 6 – RELAP5 Horizontal Flow Regime Map [33]

Each flow regime (bubbly, inverted annular, etc.) has multiple heat transfer correlations. These correlations are dependent on the vapor/gas or fluid temperatures relative to saturation. The flow regime is determined by the characteristics of the flow, including void fraction, fluid velocity, and superheated margin.

The heat transfer coefficient used in RELAP5-3D for bubbly superheated liquid is provided as equation 4.

$$H_{if} = \left\{ \begin{array}{l} \max \left[\begin{array}{ll} -\frac{k_f}{d_b}\frac{12}{\pi}\Delta T_{sf}\frac{\rho_f C_{pf}}{\rho_g h_{fg}}\beta & Plesset-Zwick \\ \frac{k_f}{d_b}\left(2.0+0.74\,\mathrm{Re}_b^{0.5}\right) & Lee-Ryley \end{array} \right] \\ +0.4\left|v_f\right|\rho_f C_{pf} F_1 \end{array} \right\} \left(a_{gf} F_2 F_3\right) \qquad (4)$$

$$= 0.0 \quad if\ \alpha_g = 0\ and\ \Delta T_{sf} \geq 0$$

Where:

H_{if} = volumetric interfacial heat transfer coefficient to the liquid phase (W/m^3-K)

k_f = thermal conductivity for the liquid phase (W/m-K)

L = characteristic length (m)

a_{gf} = interfacial area per unit volume (m2/m3) = $\dfrac{3.6\alpha_{bub}}{d_b}$

$\Delta T_{sf} = T_{sat} - T_f$

$\mathrm{Re_b} = \dfrac{(1-\alpha_{bub})\rho_f v_{fg} d_b}{\mu_f} = \dfrac{(We \bullet \sigma)(1-\alpha_{bub})}{\mu_f \left(v_{fg}^2\right)^{1/2}}$

$We\sigma = \max(We \bullet \sigma, 10^{-10})$

$\mathrm{d_b}$ = average bubble diameter $\left(= \frac{1}{2} d_{\max}\right)$

$= \dfrac{We \bullet \sigma}{\rho_f v_{fg}^2}, We = 5$

b = 1.0 (for bubbly flow)

$\alpha_{bub} = \max(\alpha_g, 10^{-5})$

v_{fg} = relative velocity = $v_g - v_f$ for $\alpha_g \geq 10^{-5}$

= relative velocity = $(v_g - v_f)\,\alpha_g 10^5$ for $\alpha_g \leq 10^{-5}$

$$v_{fg}^2 = \max\left[v_{fg}^2, \frac{We \bullet \sigma}{\rho_f \min\left(D' \alpha_{bub}^{1/3}, D\right)} \right]$$

D = hydraulic diameter

D' = 0.005 m for bubbly flow

$$F_1 = \frac{\min\left(0.001, \alpha_{bub}\right)}{\alpha_{bub}}$$

$$F_2 = \frac{\min\left(0.25, \alpha_{bub}\right)}{\alpha_{bub}}$$

$$F3 = \left\{ \begin{array}{ll} 1 & \Delta T_{sf} \leq -1 \\ \max\left[0.0, F_4\left(1+\Delta T_{sf}\right) - \Delta T_{sf}\right] & -1 < \Delta T_{sf} < 0 \\ \max\left(0.0, F_4\right) & \Delta T_{sf} \geq 0 \end{array} \right.$$

$F4 = \min[10^{-5}, \alpha_g(1-X_n)](10^5)$

X_n = noncondensible quality

The volumetric heat transfer coefficient in equation 4 (H_{if}) is based on the maximum Nusselt number produced by one of two correlations. The first correlation is derived from an analytical formulation developed by Plesset and Zwick [3]. This correlation represents the growth rate of a bubble radius. The equation as formulated here makes some simplifying assumptions. It is assumed that the bubble remains spherical throughout its growth, the radial acceleration and velocity of the interface are small, the translational velocity of the bubble is negligible, compressibility and viscous effects are negligible, and the vapor within the bubble has a uniform temperature and pressure equal to those of the interface. The second correlation was developed by Lee and Ryley [4], but modified here for use in RELAP5-3D. The modification eliminates the Prandtl number, which is 0.98 at typical reactor operating conditions. The Lee and Ryley correlation is based on observations of the evaporation rate of a water droplet suspended from a glass fiber into superheated steam flow. This correlation is somewhat limited, since it was made based on observations of droplet evaporation rather than bubble growth. It models forced convective heat transfer over a sphere, making it applicable to spherical bubbles.

The interfacial area per unit volume (a_{gf}) is required for specification of the volumetric heat transfer coefficients (H_{if} and H_{ig}). The interfacial area is computed from the diameter of the bubbles. Nukiyama and Tanasawa [5] generated a probability density function for the distribution of droplet diameter in a spray. The Sauter-mean diameter is defined as the diameter of a droplet with the same area-to-volume ratio as the entire spray (total surface area of the droplets to total volume of the droplets). Writing the Sauter-mean diameter as a ratio of integrals, and substituting the probability density function developed by Nukiyama and Tanasawa, the equation for interfacial area per unit volume (a_{gf}) shown above can be derived.

TRACE also uses the interfacial heat transfer relationships to close both the mass and energy equations. The interfacial heat transfer models consider four pre-Critical Heat Flux flow regimes as shown in Figure 2.

The bubbly flow regimes (dispersed bubble, slug flow, and Taylor cap bubble) are collectively called the "bubbly/slug" flow regime in the closure relationship development. The closure models used for the bubbly/slug and annular/mist flow regimes are applied to both vertical and horizontal geometries. The flow regime is determined based on void fraction and mass flux as shown in Figure 7. Models are used to determine

interfacial area and heat transfer coefficient based on the flow regime. The region of churn flow (transition from bubbly/slug to annular/mist) is approximated by interpolation between the values for the other regimes.

The liquid-side heat transfer coefficient between phases in bubbly flow is computed as shown in equation 5.

$$h_{li,DB} = \frac{k_l}{d_{DB}} Nu_{DB} \tag{5}$$

The Nusselt number in equation 5 is given by equation 6.

$$Nu_{DB} = 2.0 + 0.6 \cdot \mathrm{Re}_{DB}^{1/2} \cdot \mathrm{Pr}_l^{1/3} \tag{6}$$

The Reynolds number for dispersed bubbles shown in equation 6 is given by equation 7. The relative dispersed bubble velocity is given in equation 8. The diameter for a dispersed bubble is approximated by that of a distorted bubble and is a function of the Laplace coefficient. The formula is given as equation 10. The interfacial area per unit volume for the dispersed bubbles is equation 11. The volumetric interfacial area can be used with the heat transfer coefficient calculation in equation 5 to obtain an equivalent heat transfer coefficient for comparison to the volumetric heat transfer coefficient derived in the RELAP code (equation 4).

$$\mathrm{Re}_{DB} = \frac{\rho_l \cdot V_{r,DB} \cdot d_{DB}}{\mu_l} \tag{7}$$

$$V_{r,DB} = \min\left[\left|V_g - V_l\right|, V_{DB,term}\right] \tag{8}$$

$$V_{DB,term} = \sqrt{2}\left(\frac{\sigma \cdot g \cdot \Delta\rho}{\rho_l^2}\right)^{1/4} \cdot (1-\alpha)^{2.39} \tag{9}$$

$$d_{DB} = 2La = 2 \cdot \sqrt{\sigma / g\Delta\rho} \tag{10}$$

$$A'''_{i,DB} = \frac{6 \cdot \alpha}{d_{DB}} \tag{11}$$

Where:
DB (subscript) = Dispersed Bubble
$h_{il,DB}$ = Liquid-vapor interface heat transfer coefficient (W/m^2-K)
k_l = Thermal conductivity of liquid phase (W/m-K)
d_{DB} = Dispersed bubble average diameter (m)
Nu_{DB} = Nusselt number
Re_{DB} = Reynolds Number
Pr_l = Liquid Prandtl number
ρ_l = Liquid density (kg/m^3)
μ_l = Liquid phase viscosity (Ns/m^2)
$V_{r,DB}$ = Relative velocity of dispersed bubbles (m/s)
V_g = Velocity of vapor-gas mixture (m/s)
V_l = Velocity of liquid (m/s)
$V_{DB,term}$ = Terminal velocity of dispersed bubbles (m/s)
σ = Surface Tension (N/m)
g = Gravitational acceleration (m/s^2)
α = Void fraction (volume fraction of gas phase)
La = Laplace number
$A'''_{i,DB}$ = Interfacial area per unit volume (m^{-1})

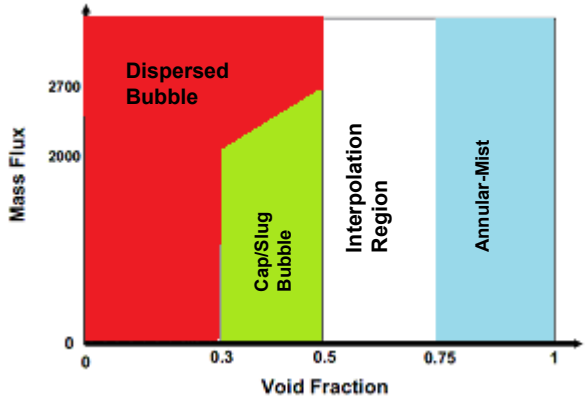

Figure 7 – TRACE Pre-CHF flow regime - interfacial heat transfer [14]

Although horizontal flows use the same flow regime map as the vertical flows, this is not always a correct assumption. Slow flows in horizontal or inclined pipes can become stratified as gravity causes the phases to separate. Figure 3 shows the horizontal flow regimes that are generally recognized. The TRACE closure relationships have been developed for the stratified smooth and stratified wavy flow regimes. As with the bubbly/slug and annular/mist regimes, the code interpolates between the stratified and vertical flow regimes.

The representative post-CHF heat transfer regimes are shown in Figure 4. The post-CHF region is defined by the bottom and top quench front seen in Figure 4. Outside of this region, the normal pre-CHF closure relationships are used. If the computational volume is partially quenched, an interpolation between the pre- and post-CHF values is used. The TRACE code models three inverted flow regimes for post-CHF conditions. These are: inverted annular, inverted slug and dispersed flow. Figure 8 shows the flow regime map for post-CHF heat transfer.

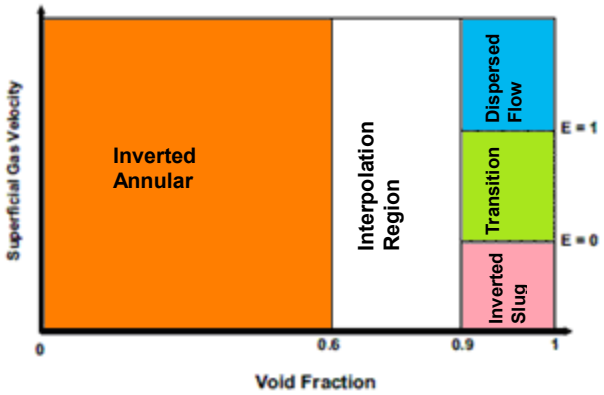

Figure 8 - Post-CHF flow regime map [14]

The interfacial heat transfer relationships that are used in the COBRA-TRAC code close both the mass and energy equations. The pre-CHF flow regimes that are recognized by the COBRA-TRAC code are shown the flow regime map in Figure 9. The computation of the interfacial heat transfer coefficient for the bubbly-slug flow regime is similar to the method for the TRACE code. The heat transfer coefficient is dependent on the thermal conductivity of the liquid, bubble diameter and Nusselt number, as shown in equation 5. The upper limit of the Nusselt number is determined in COBRA-TRAC using the liquid Prandtl number as shown in equation 12. The Reynolds-dependent Nusselt number is computed as shown in equation 13. These values for the Nusselt number can then be compared, and the smaller value is used in the calculation of the bubbly-slug interfacial heat transfer coefficient. Similar methods are used for the remaining flow regimes considered by COBRA-TRAC, including the Churn-Turbulent and annular regimes.

$$Nu_{\max} = 116.7\sqrt{\mathrm{Pr}_{liq}} \tag{12}$$

$$Nu = 2 + \left(0.4\sqrt{\mathrm{Re}} + 0.06\,\mathrm{Re}^{2/3}\right)\mathrm{Pr}_{liq}^{0.4} \tag{13}$$

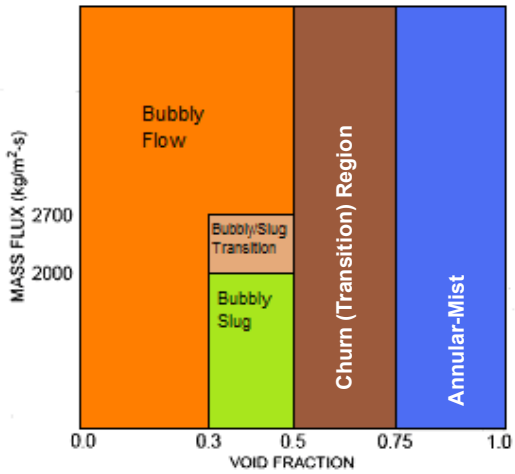

Figure 9 – COBRA-TRAC Pre-CHF flow regime - interfacial heat transfer [2]

The CATHARE code uses a heat transfer model developed from empirical data to compute the heat flux from a liquid to the interface during vaporization. The data was obtained from the SUPER MOBY DICK and the MARVIKEN tests that used long nozzles. The empirical model was selected as the standard model in CATHARE. A mechanistic model was selected for the liquid to interface heat flux under direct contact condensation. The vapor to interface heat flux model uses a laminar forced convection heat transfer model that employs a Nusselt correlation valid for a solid sphere.

The ATHLET code considers four flow regimes:

- Bubble/slug flow
- Annular and annular-mist flow
- Stratified flow
- Horizontal plug flow and vertical water level

The flow regime is determined as a function of the void fraction, phase velocities, turbulence, and inclination of the flow path. In this way, ATHLET is not unlike the other system codes. For void fractions between 0 and 0.5, the code assumes bubbly flow. For void fractions of 0.75 to 1, the annular-mist flow correlations are assumed. For void fractions falling between the two ranges, the values are interpolated. In the bubbly flow regime, the Nusselt number is computed as shown in equation 14 using the Peclet number computed as shown in equation 15.

$$Nu_B = \frac{2}{\pi^{1/2}} Pe_B^{1/2} \tag{14}$$

$$Pe_B = 2 \cdot \frac{U_B \cdot R_B}{a_L} \tag{15}$$

Where:

U_B = Bubble velocity, relative to surrounding fluid

R_B = Bubble Radius

a_L = Thermal diffusivity of the liquid ($k/\rho c_p$)

Wall-to-fluid Heat Transfer: A boiling curve (Figure 10) is used in RELAP5-3D to determine the correct heat transfer correlation from the wall surface to the fluid. Much of the logic to select the correct term is based on wall surface temperature and void fraction. All the correlations are based on fully-developed flow at steady-state, with no consideration of entrance length except for CHF calculations, since the wall geometry can also affect the heat transfer coefficients. The pre-CHF heat transfer regimes have wall-to-liquid contact. Both convection heat transfer and nucleate boiling are included in the pre-CHF regime.

By default, RELAP5-3D uses the Dittus-Boelter equation shown in equation 16 to calculate the heat transfer coefficients from the wall for turbulent, single-phase forced-convection flows. Other correlations (Gnielinski [6], Jackson [7], Petukhov [8], etc.) are available by user selection. In equation 16, C=0.023 and n=0.4 for heating or cooling. The form of equation

16 is assumed to be suitable for cooling and heating, although the derivation of the equation prescribes a value of n=0.3 for cooling. The assumption results in a 15% higher prediction of heat transfer coefficient for vapor/gas and a 10% higher coefficient for liquid at high pressures (~2,500 psia). If the fluid is at lower pressure, the error decreases significantly.

$$Nu = C \cdot \mathrm{Re}^{0.8} \cdot \mathrm{Pr}^{n} = h\frac{D}{k} \tag{16}$$

For single-phase flows, the RELAP5-3D code has correlations for the heat transfer from the wall for laminar, turbulent, and natural convection. The code selects the maximum heat transfer coefficient of the three correlations, which ensures a smooth transition between them.

The mass flux used in computing the Reynolds number for equation 16 is increased in two-phase flows (such as bubbly, annular or slug flow) with wall temperatures below the required value to cause nucleate boiling. In these cases, the liquid mass flux times the vapor/gas-to-liquid density ratio is added to the vapor/gas mass flux. This increases the Reynolds number, which has the effect of increasing the heat transfer coefficient to account for the improved heat transfer from the wall to the two-phase flow.

RELAP5-3D is limited to correlations for circular pipes. If heated parallel plates are to be modeled, an annulus can be used, since an annulus with a large inner radius has the same flow field as parallel plate flow. Heat transfer from/to spheres or any other geometries can be modeled in RELAP5-3D, but no specific heat transfer correlations are available inside RELAP5-3D for the spherical shape.

When the analysis includes forced convection, TRACE correlations specific to tube and rod bundle geometries are used. Correlations for single-phase liquid convection, two-phase forced convection, onset of nucleate boiling, nucleate boiling, and subcooled boiling are all included in the code.

As with the RELAP5-3D code, TRACE computes three wall-to-fluid heat transfer coefficients for single-phase flow. The maximum heat transfer coefficient between the laminar, natural circulation and turbulent correlation results is used to model the heat transfer from the wall to the coolant. Wall geometry is captured for each of the three regimes (laminar, turbulent and natural circulation) by different correlations.

For single-phase turbulent forced convection in tube geometry, the Gnielinski correlation is used by default in the TRACE code. Equation 17 shows the correlation for Nusselt number.

$$Nu_{turb} = \frac{(f/2)(\mathrm{Re}-1000)\cdot \mathrm{Pr}}{1+12.7\cdot(f/2)^{1/2}\left(\mathrm{Pr}^{2/3}-1\right)} \tag{17}$$

Where f is the friction factor, and other terms are as previously defined. This correlation is available in RELAP5-3D by user-selection.

The two-phase forced convection heat transfer model is used whenever the fluid is two-phase and the wall temperature is below the necessary value to cause nucleate boiling. With two-phase flow the forced convection heat transfer is improved above that of single-phase flow. In TRACE, the two-phase forced convection heat transfer coefficient is determined using an equation similar to the single phase flow heat transfer coefficient (equation 17). The modified equation for the Nusselt number is shown in equation 18, the two-phase heat transfer coefficient is dependent on the void fraction, and is shown in equation 19.

$$Nu_l = 0.0155 \cdot \mathrm{Re}_l^{0.83} \cdot \mathrm{Pr}_l^{0.5} \cdot \frac{D_h}{L} \cdot \left(\frac{\mu_b}{\mu_w}\right)^{0.33} \tag{18}$$

$$\frac{h_{2\Phi}}{h_l} = (1-\alpha)^{-0.83} \tag{19}$$

Where:

$h_{2\Phi}$ = Heat transfer coefficient for two-phase flow

h_l = Heat transfer coefficient for single-phase flow determined from the Nusselt number in equation 18

α = Void fraction (volume fraction of gas phase)

μ_b = Viscosity of "bulk" fluid

μ_w = Viscosity of the fluid at the wall temperature

$\mathrm{Re}_l = \frac{\rho_l(1-\alpha)\cdot V_l \cdot D_h}{\mu_l}$

It is apparent from equations 18 and 19 and the definition of Re_l that the effect of the correction factor (equation 19) is to adjust the Reynolds number so that it is dependent on the actual liquid velocity, rather than the superficial liquid velocity. This adjustment to the Reynolds number is very similar to what was done for the RELAP5-3D code by augmenting the liquid mass flux multiplied by the vapor-to-liquid density ratio with the vapor mass flux. This modification to the two-phase Reynolds number has the effect of increasing the heat transfer coefficient to account for the presence vapor phase.

For heat transfer to laminar two-phase flow, the Nusselt number is not a function of the Reynolds number, so it is sufficient to leave the laminar Nusselt number unmodified, and that is the case for the TRACE code. For annular flow, the modification to the heat transfer calculation uses the thickness of the annular film as the characteristic length in the calculation of the Nusselt number, instead of the pipe diameter. Equation 20 shows the equation for the annular flow heat transfer coefficient.

$$h_{wl} = \frac{k_l}{\delta} \cdot Nu_{wl} \tag{20}$$

Where:

δ = Film thickness

Nu_{wl} = Wall to liquid Nusselt number

h_{wl} = Wall to liquid heat transfer coefficient

k_l = Thermal conductivity of liquid

The film thickness in equation 20 is calculated from the void fraction as shown in equation 21. The wall to liquid Nusselt number is computed by a power-law weighting of values for laminar and turbulent flow as shown in equation 22.

$$\delta = \frac{D_h}{2} \cdot \left(1 - \sqrt{\alpha}\right) \tag{21}$$

$$Nu_{wl} = \left(Nu_{lam}^2 + Nu_{turb}^2\right)^{1/2} \tag{22}$$

The laminar Nusselt number from equation 22 is computed as shown in equation 23. The turbulent Nusselt number is shown in equation 24.

$$Nu_{lam} = 2 \cdot \left(1 + 1.83 \times 10^{-4} \cdot \mathrm{Re}_f\right) \tag{23}$$

$$Nu_{turb} \approx \frac{1}{4} Nu_{Gnielinski} \tag{24}$$

The $Nu_{Gnielinski}$ correlation is the same as that shown in equation 17. Equation 24 results from the understanding that the hydraulic diameter of a thin liquid film is four times the film thickness. The Reynolds number for a film (Re_f) is defined as shown in equation 25.

$$\mathrm{Re}_f = \frac{4 \cdot \Gamma_f}{\mu_l} \tag{25}$$

In equation 25, Γ_f is the film flow rate per unit width of the wetted perimeter of the annular film. This completes the TRACE model for heat transfer to an annular flow regime from the wall.

TRACE has an additional film condensation heat transfer model that is used whenever the surface temperature of the wall is less than the saturation temperature at the vapor partial pressure and the void fraction is greater than 90%. If the void fraction is less than 80%, the normal two-phase convection models are used. If the void fraction is between 80 and 90%, the heat transfer coefficient is interpolated between the values obtained for two-phase convection and film condensation.

The wall heat transfer in CATHARE is modeled in much the same way as described for the RELAP and TRACE codes. The Pre-CHF heat transfer uses the classic Colburn correlation for forced convective heat transfer to the liquid.

The TRAC code uses the Dittus Boelter correlation to compute the single-phase heat transfer coefficient from the wall to a turbulent flow. TRAC uses the Chen correlation [9] extended for nucleate boiling to compute the heat transfer coefficient when the wall surface temperature exceeds saturation, but does not reach the temperature for CHF. The heat transfer coefficient (HTC) is computed as the sum of the "forced circulation" HTC and the "nucleate boiling" HTC. The forced circulation HTC is essentially the Dittus Boelter correlation with an additional factor to account for the property variation between phases. The nucleate boiling HTC is computed as shown in equation 26. The sum of the HTC terms is used for nucleate boiling. The suppression factor, S_{CHEN}, "turns off" the nucleate boiling component of the heat flux as the flow transitions to the annular regime and the heat transfer mode becomes more dependent on convection.

$$h_{NB} = 0.00122 \cdot S_{CHEN} \left(\frac{k_l^{0.79} C_{p,l}^{0.45} \rho_l^{0.49} g_c^{0.25}}{\sigma^{0.5} \mu_l^{0.29} H_{fg}^{0.24} \rho_v^{0.24}} \right) \left(T_w - T_l\right)^{0.24} \cdot \left(P_w - P\right)^{0.75} \tag{26}$$

Where:
S_{CHEN} = Boiling suppression factor [9]
k_l = Thermal conductivity of liquid
$C_{p,l}$ = Specific heat of liquid phase
ρ_l = Density of liquid phase
g_c = Gravitational conversion factor (ft-lbm/lbf-hr^2)
σ = Surface tension
μ_l = Viscosity of liquid phase
H_{fg} = Heat of formation
ρ_v = Density of vapor phase
T_w = Temperature of wall
T_l = Temperature of liquid
P_w = Saturation pressure corresponding to T_w
P = Pressure of coolant.

The ATHLET code uses the same Chen correlation and adjustments that were used in TRAC to compute the nucleate boiling heat transfer coefficient.

CHF Correlations: The CHF point is defined as the maximum heat flux on the boiling curve shown in Figure 10. The CHF point marks the transition between wetted-wall heat transfer regimes like nucleate boiling, and the post-CHF regimes like transient or film boiling. The calculation of the CHF point in RELAP is used to determine the heat transfer regime that should be used (either pre- or post-CHF).

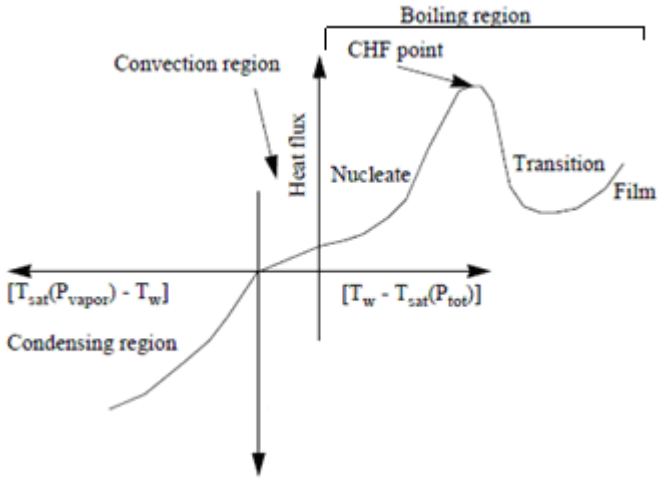

Figure 10 - Boling Curve [33]

The PG-CHF correlation in the RELAP5-3D code is a newly implemented set of CHF correlations that were developed by the Nuclear Research Institute Rez in the Czech Republic [10, 11]. The correlations are based on data in the Czech Republic data bank from 173 different sets of tube data, 23 sets of annular data, and 153 sets of rod bundle data. These closure relations are used to determine the onset of CHF. Once CHF is reached, the RELAP code uses the Chen transition boiling model [12] to compute the heat transfer from the wall to the coolant.

The Critical Heat Flux (CHF) model in TRACE serves much the same purpose as the model used in the RELAP5 code. The temperature of the CHF point is important in the determination of the transition of the heat transfer regime (from pre-CHF to post-CHF/dryout). However, unlike the RELAP code, the CHF point (see Figure 11) is also used to provide an upper bound on the transition boiling region heat transfer. The default model to determine the point of CHF is the 1995 AECL-IPPE look-up table. This table is based on an extensive CHF database obtained in tubes with a vertical upflow of a steam water mixture. The correlation provides a value for critical heat flux as a function of local conditions. A correction factor is used to improve the accuracy when applied to rod bundles.

The minimum film boiling temperature (T_{min}, Figure 11, also known as the Leidenfrost point) provides a lower bound for the transition boiling heat flux. The minimum film boiling temperature represents the point where the heat transfer regime switches from transition boiling to film boiling. These two points are used in the TRACE code to define the transition boiling heat transfer regime. The heat transfer based on wall superheat is determined by interpolation between these two points. The same interpolation approach used in COBRA-TRAC was used in TRACE.

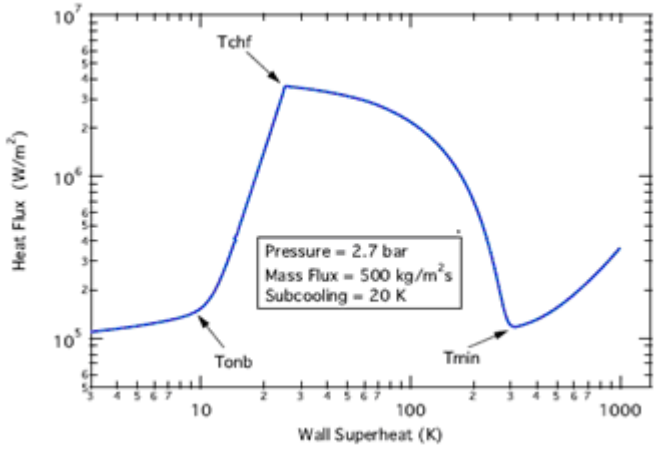

Figure 11 - TRACE Boiling Curve [14]

The minimum film boiling temperature is determined using the Groeneveld-Stewart correlation [13,14]. This empirical correlation determines the minimum temperature over a wide pressure range. It is based on vapor film collapse data.

The post-CHF regimes (see Figure 8) are often called "inverted" flow regimes because the liquid is not in contact with the wall due to elevated surface temperatures. TRACE includes correlations for inverted annular film boiling, dispersed flow film boiling, and inverted slug film boiling. Heat transfer coefficients for each of these regimes are determined from empirical correlations for the Nusselt number based on measured data.

The model of transition boiling in CATHARE relies on the adequate prediction of the CHF point. The table proposed by Groeneveld is used to compute CHF based on pressure, quality and mass velocity. Correction factors are applied for rod bundles. The transition boiling heat flux is derived from a parabolic interpolation between the CHF temperature and the minimum temperature. The minimum temperature is based on the Groeneveld-Stewart correlation. This technique is similar to what was done for the TRACE code as previously described. In the post-CHF flows, three heat transfer mechanisms are considered: radiation heat transfer from the surface to the vapor and liquid, convective heat transfer from the wall to the vapor, and convective heat transfer from the vapor to the liquid interface. These three mechanisms are modeled individually to capture the heat transfer to the post-CHF (dryout) flow regimes.

As in the TRACE code, TRAC uses the minimum film boiling temperature (Tmin) to determine the upper limit of the transition boiling region. The model for heat transfer from the wall to the coolant in the transition boiling region is developed from the assumption that transition boiling is composed of nucleate boiling (wet wall) and film boiling (dry wall) components. The heat transfer equation (equation 27) comes from Bjornard and Griffith [15].

$$q''_{TransBoil} = F_{wet} q''_{CHF} + (1 - F_{wet}) q''_{\min} \quad (27)$$

Where:

Fwet = Fraction of the wall area that is wet

Although it also calculates the minimum film boiling temperature, ATHLET uses a simpler method to determine if the flow is in transition boiling. The transition region after departure from nucleate boiling is determined if the wall temperature is greater than the fluid temperature and the critical heat flux temperature (T_{CHF}), but less than T_{CHF}+10K. After a departure from film boiling, the transition boiling region is defined when the wall temperature is between the return to nucleate boiling temperature (T_{RNB}) and the rewetting temperature (T_{REW}) [16]. The minimum film boiling temperature in ATHLET is used to determine when the flow regime changes from transition boiling to the post-CHF regimes.

Reflood Model: Reflood refers to the third step in the Loss of Coolant Accident (LOCA) Transient when the Emergency Core Cooling (ECC) system is activated following a LOCA. The reflood model must be efficient at low flow and low pressure boundary conditions. The flooding/quenching

conditions require modifications to the wall heat transfer coefficients that are developed for the wall-to-fluid heat transfer models. Additionally, the interfacial heat transfer and drag are also modified for reflood conditions.

The Paul Scherrer Institute (PSI) developed more advanced reflood models than previous RELAP5 versions. The advanced models improve the behavior of the quench front during reflood in the core. A modified version of this model was included in RELAP5-3D, along with the capability to plot the quench front.

The TRACE code utilizes a fine-mesh rezoning technique during reflood calculations. The model inserts transitory nodes to account for the axial gradients encountered in the quenching region.

The ATHLET code adopts one of two approaches for modeling reflood conditions. The first is to use the existing models for the heat transfer coefficient for post-CHF regimes. This model is most applicable for high pressure conditions, such as the early rewet during the blowdown phase of a large break LOCA. The second approach uses analytical correlations that take into account axial heat conduction in the cladding and pre-cooling of the dry rod surface near the quench front to determine the upper and lower quench front conditions in the reflood phase of a LOCA. The quench front locations are used to define where the change between wet and dry wall occurs. The heat transfer for the section of the wall that is wet is computed using the same methods for pre-CHF heat transfer from the wall. The dry wall section uses the post-CHF wall heat transfer calculations.

TRAC and CATHARE do not have specific reflooding models, and use the correlations for pre- and post-CHF heat transfer coefficients to compute the heat transfer during reflood.

Wall-to-wall Radiation: The wall-to-wall heat transfer is computed in RELAP5-3D using a purpose-developed heat structure (radiation enclosure). The wall to wall radiation heat transfer model is significant during post-CHF conditions between blowdown and reflooding. In order to predict the wall to wall radiation correctly, the absorption and emsissivity coefficients, along with the view factors between each wall must be close to the actual values. Most of the system codes use a pipe or annular pipe approach, and approximate view factors are used to represent the real system. This is a major assumption in the calculation of wall to wall heat transfer by radiation. In addition, the model does not include absorption by the fluid between the surfaces.

TRACE includes a similar model for the effects of radiation heat transfer. The model includes rod-to-rod and rod-to-wall radiation, as well as wall-to-fluid. The rod-to-wall or rod-to-rod radiation heat transfer model is selected as a user option, although the default model only includes wall-to-fluid radiation.

CATHARE includes a wall-to-wall radiation heat transfer model that was developed for RBMK core channels, and includes the corresponding view factors. Alternate core geometries can be modeled if the view factors are input appropriately [17].

ATHLET assumes that all emissive surfaces are gray, that radiative heat transfer is calculated on the basis of a plain approach where all bodies are treated as infinitely long cylindrical bodies, and radiative heat transfer is only considered for flow regimes with high void fraction in the core channel. As with CATHARE, the view factors for the RBMK core channels are built in to the code, but other core geometries can be used if the correct view factors for the core are input correctly [17].

The TRAC code limits radiation heat transfer between surfaces to the radiation heat transfer from the rods to the grid. No additional models are available for radiation heat transfer between user-defined surfaces.

Energy Source Term: This model captures direct heating of the fluid as a percentage of the heat generated in the heat structure. This effectively captures the effect of neutron heating in the reactor coolant. This relationship provides an energy deposition source term to the energy conservation equations.

RELAP/SCDAP can also model heat generation due to chemical interactions. Severe accident scenarios that result in clad-water interactions can be modeled using these models.

This capability is not present in TRACE, COBRA-TRAC, CATHARE, or ATHLET.

Momentum Closure Relationships

The RELAP5-3D momentum equation closure relations include:

- Interphase friction
- Wall drag relationships
- Entrainment correlation

The interphase friction used more than one approach to determine the friction at the interface between the phases. The drift flux model is used in the bubbly and slug-flow regimes for vertical flow. The drag coefficient model is used in all the remaining flow regimes.

The wall drag relationships capture the pressure loss due to wall shear from cell center to cell center of the cell volumes adjoining the junction that is under evaluation by the momentum equation. The wall drag depends on the phase of the fluid and on the flow regime characteristics. The phasic wall friction coefficients are determined from the Darcy-Weisbach equations, apportioning the overall wall frictional pressure gradient between the phases.

The entrainment correlation is used in the annular-mist flow regime to calculate the wall to coolant heat transfer by proper apportioning of the liquid in the wall region as an annular film and in the vapor/gas region as droplets. The code uses the Ishii and Mishima correlation [18, 19] for entrainment fraction as a basis for calculating the liquid volume fraction fractions in the film and vapor/gas regions.

The closure relations for RELAP5-MOD3 are very similar to those used in RELAP5-3D, but it does not have several of the wall to liquid heat transfer models that are available in RELAP5-3D. The missing correlations are for additional arrangements of rods (in-line or staggered) and with or without

crossflow. Also, RELAP5-MOD3.3 does not have a closure relationship for swirl tubes, which RELAP5-3D includes.

The closure relations for RELAP5-MOD3 are very similar to those used in RELAP5-MOD3.3, but it does not have the PG-CHF correlations or a reflood model. In place of the PG-CHF correlations, a lookup table method is used. RELAP5-MOD3 also lacks the same wall to liquid heat transfer models that are available in RELAP5-3D.

At this stage of the RELAP7 development, a full implementation of the closure models is unnecessary. Since RELAP7 is currently limited to modeling single-phase flows, the additional closure relations are not yet needed. However, the closure models used in RELAP5 and other newly developed models will be considered when it becomes necessary to provide closure models to RELAP7.

The SCDAP code is applied to the RELAP code as an extension of the RELAP code capability. SCDAP is predicts fuel performance, chemical interactions and severe accident conditions. Several versions of RELAP-SCDAP have been developed, but in every case, the hydraulic modeling of the coolant channels is essentially identical to the version of RELAP used as the base code. Thus, the closure models are largely the same as those used in RELAP, though additional models are implemented to account for the relocation of fission products, fuel, cladding, etc. during severe accidents. The heating generated by oxidation of the control rods is also modeled by closure relationships.

There are only two flow pattern transitions that are modeled in the CATHARE closure laws. These are the stratification limit and the onset of entrainment. Three correlations are used: one for stratified flows, one for droplet entrainment, and a third for non-stratified flows with no entrainment. The third correlation covers the entire range of bubbly, slug, churn and annular flows. The interfacial friction for non-stratified flows with moderate void fraction and no entrainment are assumed to be bubbly, slug and churn flows. Drift flux models are used to correlate these flow regimes. CATHARE includes drift flux models for rod bundles, pipes, and annuli. The Wallis friction coefficient for annular flows can be applied to stratified flows. In droplet flows, the interfacial friction correlations require a correct estimate of the droplet diameter. Correlations for calculating the droplet diameter are included in CATHARE, but only one diameter value (based on cross sectional flow area, superficial tension, and vapor velocity) is considered in the model.

Closure of the conservation equations in COBRA-TRAC is achieved using normal thermodynamic relationships and additional specifications for interfacial drag coefficients, interfacial heat transfer, phase change rate, wall-shear coefficients, and wall heat flows [2]. Closure relations for a transient eliminate the necessity of a quasi-steady assumption, but unique relations may be required for every transient [20]. The phase change rate evaluated from thermal-energy-jump relation. Newton's law of cooling is used to determine the heat transfer from the wall.

The liquid and vapor field momentum equations in TRACE include terms for the interfacial shear and wall drag forces. The closure relations used are dependent on flow regime, and include interphase friction and wall drag relationships that are required for closure. These closure relations can be characterized as:

- Pre-CHF interfacial drag models
- Stratified flow interfacial drag models
- Post-CHF interfacial drag models
- Single-phase friction factor
- Pre-CHF regime wall drag
- Wall drag with horizontal stratified flow
- Post-CHF flow regime wall drag

The pre-CHF regimes considered for interfacial drag are Bubbly/Slug and Annular/Mist. The models used for the drag in these regimes are applied to both vertical and horizontal flows, as was the case for the interfacial heat transfer models. There is no explicit flow regime map for interfacial shear determination. The two regimes are individually considered and combined using a simple power law weighting scheme [14]. The drift flux model is used in the bubbly/slug flow regime. The formulation of the model includes correlations for pipes and bundles. The correlation for the annular/mist regime combines interfacial drag for an annular film with that for entrained droplets.

Not all of the stratified flow regimes shown in Figure 3 are explicitly modeled in TRACE. The dispersed bubble and annular/dispersed regimes are modeled using the comparable vertical flow regimes without modifications to account for the horizontal flow condition. The stratified wavy and plug/slug flow are also not explicitly modeled in TRACE. They are treated as transition regimes when a horizontal flow is changing from a non-stratified flow to a stratified flow. The transition is modeled using an exponential weighting scheme. This leaves the stratified smooth regime as the only one that is explicitly considered for interfacial drag calculations. In order to be considered stratified flow, the component must have an inclination angle less than 80 degrees, and must not have vertical junctions at both ends. The interfacial friction factor is computed using the Ohnuki et. al. correlation [21].

The interfacial drag in post-CHF flow regimes in TRACE is modeled for three inverted regimes. They are the inverted annular, inverted slug, and dispersed flow. Figure 8 shows the regions over which each of these regimes is used.

The wall drag closure relationships in TRACE apply to single-phase flow, pre-CHF two-phase flow, horizontal stratified flow, and post-CHF two phase flow.

For single-phase flow, the wall friction factor in TRACE is defined using the Churchill formula [22], which applies to a wide range of flow regimes (laminar, transition, and turbulent). The friction factor from the Churchill equation is used in the wall drag coefficient [14].

The pre-CHF regimes considered for wall drag are bubbly/slug and annular/mist, as before. The drag on the vapor phase is neglected, so all the wall drag is applied to the vapor phase. The two-phase multiplier and friction factor are

computed to determine the effect of the wall drag on the fluid phase alone.

In horizontal stratified flow, both liquid and gas phases are in contact with the wall. The TRACE code applies the wall drag coefficient to both phases. The wall shear stress model is from Taitel and Dukler [23], and the shear stress is defined for the liquid and gas phases separately. The friction factors are evaluated for each phase for both laminar and turbulent flow. The friction factors are those for simple pipe flow, so the Churchill formula is again used to compute the wall drag. The same criteria as were used for the horizontal interfacial shear calculations are again used to determine if the flow is stratified.

The gas phase is in contact with the wall for the post-CHF flow regimes. Therefore, only the wall drag for the gas phase applies to the post-CHF regimes. The wall drag on the liquid phase is zero. The inverted annular regime is treated as a direct analog to the annular regime. The frictional pressure gradient for the dispersed flow regime is computed using a model for particle-laden flows developed by Pfeffer et. al. [24].

TRACE closure relationships model the heat and mass transfer between phases for each of these flows and temperature regimes. The interfacial mass transfer rate per unit volume is computed as the sum of mass transfer rates from interfacial heat transfer and subcooled boiling. As with the RELAP code, the applicable flow regime is determined by void fraction, velocity, and temperature. TRACE computes the CHF over a wide range of conditions using the 1995 AECL-IPPE CHF look-up table [14]. As with RELAP5-3D, models are included to account for noncondensible gasses.

There are two types of control volumes in ATHLET: an "ordinary" control volume that has a homogeneous distribution of mass and energy, and a "non-homogeneous" control volume that includes a mixture level model. The mixture model allows a boundary with steam that may include entrained droplets on one side, and liquid with entrained bubbles on the other. This is a much-simplified approach to the analysis of the flow field.

NUMERICAL SOLUTION

The system of equations that result from the conservation equations and closure relationships must be solved numerically. The solution methods can be compared by methods of discretization and by the matrix solver that is implemented. The numerical solution methods influence the performance of the codes in terms of code speed, as well as code time step requirements. Different solution schemes place different restrictions on the models.

Discretization and Time Stepping

Code speed in RELAP5-3D is improved by limiting use of implicit numeric evaluation to terms important to sonic wave propagation and phenomena with small time constants (e.g. velocity in the mass and energy transport terms, pressure gradient in the momentum equations, interface mass and momentum exchange terms).

Additional computing speed improvement is achieved by selecting time-level evaluations so that resulting implicit terms are linear in the new time variables. Taylor series expansions about the old time values are developed to retain nonlinearities and obtain a formulation that is linear in the new time variables. The linear formulation eliminates the need to iteratively solve systems of nonlinear eqns.

RELAP5-3D has a nearly-implicit option that allows violation of the courant limit. In general, this numeric scheme is suitable for steady-state calculations and quasi-steady transients. This scheme is based on a fractional step (multiple step) method. The equations are split into fractional steps that are based upon physical phenomena. The nearly-implicit scheme has two steps. The first step solves all seven conservation equations, treating the interface exchange process, pressure propagation process and momentum convection process implicitly. The finite-difference versions of the conservation equations used in the nearly-implicit solution method are exactly the same as the expanded equations solved in the semi-implicit scheme, except that the convective terms are evaluated implicitly (in linearized form) instead of in an explicit donored fashion (as in the semi-implicit scheme). The second step solves the unexpanded form of the mass and energy equations using the final junction velocities and interface exchange terms resulting from the first step. The interface heat and mass exchanges are computed using the partial solution from the first step [25].

The difference equations are built on a staggered mesh, where scalar properties (such as pressure, specific internal energies and void fraction) are defined at cell centers and vector quantities (such as velocities) are defined on cell boundaries.

The same techniques to improve calculation speed that were described in RELAP5-3D are used in RELAP5-MOD3 and MOD3.3. These versions of RELAP5 have a partially-implicit (semi-implicit/convection-explicit) finite-difference numerical scheme. The finite difference equations are partially implicit in time. There is no nearly-implicit option available in either RELAP5-MOD3 or MOD3.3. Just as with RELAP5-3D, the difference equations are built on a staggered mesh with scalar properties defined at cell centers and vector quantities defined on cell boundaries.

The RELAP7 code will eventually use the Discrete Equations Method (DEM) as the basis for the 7-equation model. This method is described in greater detail in Reference [1]. The DEM model is not yet implemented in the RELAP7 code. The 7-equation model described in [1] is explicit. A fully implicit treatment will have to be developed to reduce timestep restrictions.

RELAP-SCDAP solves the thermal-hydraulic calculations in the same way as the RELAP5-3D code. SCDAP treats the thermal properties and heat source terms implicitly. The updated temperature at current time level is used to compute the updated thermal properties and heat source, and the difference equations are solved again to give an updated temperature. The

iterations are terminated when the temperature change is small. Heat sink terms are treated explicitly [26].

The hydrodynamic calculations are computed using the RELAP5-3D methods, with the same staggered mesh techniques described previously.

The finite difference scheme in the SCDAP model uses a slightly different technique than that of the RELAP codes. SCDAP has a 2D heat conduction model. The mesh point is placed at the finite volume boundary or interface between material layers. This improves accuracy at the boundary, but means that the control volume surrounding a point may overlap mesh cells that lie in different material layers.

The semi-implicit method works well in propagating information about sound waves. For the TRACE code, a correction step was devised to propagate information for continuity waves. This technique is called the stability-enhancing two-step (SETS) method. The SETS method eliminates the courant stability limit with minimal changes. For example, consider a single-phase mass equation. For each time step the semi-implicit method is used to establish the new time velocity field. Then a stabilizer step is used to get a final value of the new time density. The density change information in any computational cell is propagated to all other cells within the same time step, and a correction step is devised for each of the mass, momentum, and energy equations. Mass and energy equations do the semi-implicit step first, then the corrector step. The momentum (motion) stabilizer equation is evaluated before the semi-implicit equations. Computational time is reduced by not computing temperatures and pressures that are fully consistent with densities and energies obtained from solving stabilizer mass and energy equations. The values for temperature and pressure that are used are those obtained during the semi-implicit equation step.

The momentum equation solution is identical to the semi-implicit method, but stabilizer velocities are used for momentum transport. For the solution to the mass and energy equations, the void fraction and new-time thermodynamic variables are intermediate results. Final new-time values are set by the stabilizer mass and energy equations, which are solved after the mass and energy equations. Final new-time values are only computed for void fraction, macroscopic densities and macroscopic energies. The thermodynamic equation of state is not used after the stabilizer mass and energy equations are solved. When basic thermodynamic variables are needed to evaluate viscosity or heat transfer coefficients, the values from the previous semi-implicit step are used to save computational time.

Similar to RELAP, a staggered mesh is used for 1D components, where velocities are defined at mesh-cell interfaces and pressure, gas volume fraction, temperatures, internal energy, and density are defined at mesh-cell centers. Scalar field equations (mass and energy) apply to a mesh cell, while velocity component motion equations apply to the interface between mesh cells in the three velocity-component directions.

In ATHLET, a finite-volume approach is used to bound the conservation equations for solution. The mass and energy equations are solved within control volumes, while the momentum equations solved over junctions between control volume centers. Thus, pressures and temperatures are solved at cell volume centers, and velocities are solved at volume junctions.

CATHARE discretizes all the terms in the six equation model and the closure relationships fully implicitly in 1D (e.g. pipes) and 0D (boundary condition) components and semi-implicitly in 3D (vessel) components. The discretization includes mass exchange between phases, as well as the pressure and convection terms. The non-linear equations that result are solved using iterative Newton solver methods. The CATHARE code supports multiple processors.

In COBRA-TRAC, the finite-difference equations are written in a semi-implicit form using donor cell differencing for convected quantities. The timestep is limited by the material Courant limit. As with the other codes considered, the pressures and temperatures are computed on cell centers, and the velocity and other vector quantities are computed on the cell boundaries.

Matrix Solution

In RELAP5-3D, the equations are formed into a linear time-advancement matrix that is solved by direct inversion using a border-profile lower upper (BPLU) solver [25]. The BPLU solver is used to efficiently solve sparse linear systems of the form AX = B. It is designed to take advantage of pipelines, vector hardware, and shared-memory parallel architecture to run fast. BPLU is most efficient solving systems that correspond to networks, such as pipes, but it is efficient on any system that can be permuted into border-banded form. BPLU is an efficient direct LU factorization scheme that minimizes both fill-in and wasteful operations with zero. The sparse-matrix solver can also be used based on user-input.

Implicit terms are formulated to be linear in the dependent variables at the new time in RELAP5-MOD3 and –MOD3.3. The linear time-advancement matrix is solved by direct inversion using a sparse-matrix routine. The BPLU solver is not available in RELAP5-MOD3 or –MOD3.3 The direct inversion using the sparse-matrix routine is the only solution method available.

The current version of RELAP7 uses a JFNK nonlinear solution scheme that is second order accurate in time and space to solve the mass, momentum, and energy equations for 1D, single-phase flow. The finite-element mesh is managed by the Multiphysics Object-Oriented Simulation Environment (MOOSE) application under development at the INL. MOOSE is a simulation framework that facilitates computer simulation from complex mathematical models.

The RELAP-SCDAP code uses the alternating direction implicit (ADI) numerical scheme [27] is used to set up the tridiagonal system of equations that are solved using Gaussian elimination or odd-even reduction methods.

